Electron momentum density of TTF-TCNQ (tetrathiafulvalene-tetracyanoquinodimethane) studied by Compton scattering

1999 J. Phys.: Condens. Matter 11 9025

(http://iopscience.iop.org/0953-8984/11/46/305)

J. Phys.: Condens. Matter **11** (1999) 9025–9032. Printed in the UK PII: S0953-8984(99)07477-9

Electron momentum density of TTF-TCNQ (tetrathiafulvalene-tetracyanoquinodimethane) studied by Compton scattering

Shoji Ishibashi†‡, Alfred A Manuel†, Dharmavaram Vasumathi†, Abhay Shukla§, Pekka Suortti§, Masanori Kohyama‖ and Klaus Bechgaard¶

† Département de Physique de la Matière Condensée, Université de Geneve, 24 quai E Ansermet, CH-1211 Geneva 4, Switzerland
‡ Electrotechnical Laboratory, 1-1-4 Umezono, Tsukuba, Ibaraki 305-8568, Japan
§ High-Energy group, ESRF, BP 220, F-38043 Grenoble, France
‖ Department of Material Physics, Osaka National Research Institute, AIST, 1-8-31 Midorigaoka, Ikeda, Osaka 563-8577, Japan
¶ Condensed Matter Physics and Chemistry Department, Risø National Laboratory, PO Box 49, DK-4000 Roskilde, Denmark

Received 1 September 1999

Abstract. We have investigated the electronic structure of the quasi-one-dimensional organic metal TTF-TCNQ by measuring Compton scattering from single crystals. The measured profiles are significantly anisotropic. The directional anisotropies were compared with those derived by two different theoretical approaches. The first is the molecular orbital approximation: Compton profiles were calculated for the TTF and TCNQ molecules, separately, and then these were superposed. In spite of the simplicity of this approach, the agreement is reasonably good, implying that the electronic wave functions of TTF and TCNQ in the crystal are not very different from those of isolated molecules. The second approach is an *ab initio* pseudopotential band-structure calculation. The agreement is better, presumably due to the more accurate description of the crystallinity (including, for example, the inter-molecule charge transfer and band formation).

1. Introduction

With the availability of large synchrotron radiation facilities providing intense hard x-ray beams, the resolution of the Compton-scattering technique has been drastically improved [1]. This technique can nowadays be efficiently applied to the study of the electron momentum densities in condensed matter. It allows a direct measurement of the total amplitude of the electron wave functions in momentum space, as the Compton profile $J(p_z)$ is the one-dimensional projection of the total electron momentum density $\rho(\boldsymbol{p})$:

$$J(p_z) = \int_{-\infty}^{\infty} \rho(\boldsymbol{p})\, \mathrm{d}p_x\, \mathrm{d}p_y \tag{1}$$

where p_z is parallel to the scattering vector. Among a number of interesting materials which may be investigated by Compton scattering, organic metals are particularly well suited because they are made of low-Z elements and have low volume densities.

0953-8984/99/469025+08$30.00

Tetrathiafulvalene-tetracyanoquinodimethane (TTF-TCNQ: $C_{18}H_8N_4S_4$) is a quasi-one-dimensional organic conductor at temperatures above 58 K [2,3]. It was the first organic metal to be synthesized. The TTF skeleton is the generic structure for many organic superconductors such as TMTSF and BEDT-TTF salts [4, 5]. Therefore, TTF-TCNQ is an important material, both historically and scientifically.

TTF-TCNQ consists of homologous stacks of TTF and TCNQ molecules arranged in a monoclinic crystal structure containing two chemical formula units within the unit cell [6]. At room temperature, 0.55 electrons per molecule are transferred from the highest occupied molecular orbital (HOMO) of TTF to the lowest unoccupied molecular orbital (LUMO) of TCNQ [7]. The quasi-one-dimensional metallic conductivity of this compound results from this charge transfer and from the crystal structure.

In the present work, we have investigated the electronic structure of TTF-TCNQ by Compton scattering. We measured Compton-profile spectra along three different crystallographic axes and obtained their anisotropies. In order to interpret the experimental results for such a complex material, theoretical support is necessary. A simple and reasonably good way to estimate the momentum density was proposed by Chiba [8, 9]. In oxides, where localized orbitals play an important role, Chiba approximated electronic wave functions with the LCAO-MO (linear combination of atomic orbitals–molecular orbitals) technique and obtained successful results. For TTF-TCNQ also, owing to its molecular crystal nature, one can expect this molecular orbital approach to be adequate to describe the electronic structure. In fact, the tight-binding approximation has been frequently applied to the calculation of the electronic structure of this compound and similar materials with success [4, 5, 10]. In addition to these molecular orbital calculations, we have performed a band calculation on the crystal state. Inter-molecular interactions, which are neglected in the LCAO-MO calculations, are now taken into account. The comparison of the results obtained with those from the two approaches illustrates the electronic structure variations involved with the crystallization.

2. Experimental procedure

The Compton profiles were measured using the high-resolution scanning spectrometer at ID15B at the ESRF [1]. The incident energy was 30.72 keV from a Si(111), cylindrically bent, focusing Bragg monochromator. The radiation scattered at an angle of 171.6° was analysed by a cylindrically bent Si(400) analyser. Single crystals of TTF-TCNQ were stacked appropriately either for the transmission or the reflection geometry. Directional Compton profiles along three principal crystallographic directions ($\boldsymbol{a}$, $\boldsymbol{b}$ and $\boldsymbol{c}^*$, perpendicular to $\boldsymbol{a}$ and $\boldsymbol{b}$; the * symbol is used for the reciprocal-lattice vectors) were measured at room temperature with high statistics (0.1% standard deviation). The final resolution at the Compton peak was 0.16 au for the a- and b-directions, where the measurements were made in the symmetric transmission mode, and 0.13 au for the c^*-direction where the measurements were made in the symmetric reflection mode. The energy transfer at the Compton peak was 3.28 keV. The incident beam was monitored using a Si PIN diode and this was used to normalize the scanned profiles. The raw profiles were further corrected for geometrical effects, for absorption in air and in the sample and for the analyser reflectivity. The background was measured separately and subtracted. Finally the profiles were folded around the origin and normalized to the correct number of electrons, using the theoretical prediction and taking into account the finite range measured in momentum space. The directional anisotropies were obtained by subtracting one profile from another.

3. Calculation

3.1. Molecular orbital calculation

In this model, the electron wave functions are expressed as superpositions of molecular orbitals from independent TTF and TCNQ molecules. We made molecular orbital calculations with two different methods. One is the Hartree–Fock method and the other is the LDA (local density approximation) pseudopotential method with the supercell technique.

3.1.1. The Hartree–Fock method. Self-consistent Hartree–Fock calculations have been performed using *Gaussian 94* [11]. Molecular orbitals are expressed as linear combinations of Gaussian-type basis functions, which are convenient for describing localized 2p and 3d orbitals. Once the molecular orbital wave functions $\psi_j(\boldsymbol{r})$ (j: molecular orbital label) are obtained, the wave functions in momentum space $\psi_j(\boldsymbol{p})$ are calculated by Fourier transformation:

$$\psi_j(\boldsymbol{p}) = \int \psi_j(\boldsymbol{r}) \exp(-\mathrm{i}\boldsymbol{p}\cdot\boldsymbol{r})\,\mathrm{d}\boldsymbol{r}. \tag{2}$$

The partial momentum density $\rho_j(\boldsymbol{p})$ corresponding to each molecular orbital j was expressed as the square of the momentum wave function:

$$\rho_j(\boldsymbol{p}) = |\psi_j(\boldsymbol{p})|^2. \tag{3}$$

The total electron momentum density $\rho(\boldsymbol{p})$ was then obtained by summing these partial densities:

$$\rho(\boldsymbol{p}) = \sum_j n_j \rho_j(\boldsymbol{p}). \tag{4}$$

The occupation number n_j is 2 except for the HOMO of TTF and the LUMO of TCNQ. Due to the charge transfer of 0.55 electrons [7], bands derived from these orbitals are not fully occupied. To account for this effect, the Fermi surface has been introduced [12] at the position which is consistent with this charge transfer. The expected break is smaller than 1% of the peak of $\rho(\boldsymbol{p})$. Finally, the calculated Compton profiles $J(p_z)$ were obtained along the crystallographic axes a, b and c^* according to equation (1). Their anisotropies were also calculated by subtracting one from another.

We have performed these calculations for four of the most frequently used analytical Gaussian basis sets: STO-3G [13], 3-21G [14], 6-31G [15] and 6-31G** [16]. Here, STO-3G means that the Slater-type orbital is constructed from a fixed linear combination of three (contracted) Gaussians. 3-21G means that each core orbital is represented by a single Slater-type orbital described by three contracted Gaussians while each valence orbital is represented by two Slater-type orbitals, one described by two contracted Gaussians and the other described by a single Gaussian. One '*' in 6-31G** means that polarization functions (here, d-type) are added to all atoms except H and the second '*' means that a p-type polarization function is added to H atoms. Among these basis sets, 6-31G** is expected to give the most accurate results.

3.1.2. The LDA pseudopotential and supercell method. In this approach, as in usual band calculations, we assume a periodic repetition of the unit structure. One TTF or TCNQ molecule is put at the centre of a 'supercell', which should be determined such that a molecule is well separated from its neighbours. Here, we used the double crystal unit cell ($a \times 2b \times c$) as the supercell. We used the same pseudopotential and plane-wave cut-off energy as the band calculation described below. 16 $\boldsymbol{k}$-points in the 1/2 Brillouin zone for the supercell were used.

To obtain the self-consistent charge density, one $\boldsymbol{k}$-point is enough. These numbers of $\boldsymbol{k}$-points were required to obtain the Compton profile. Once the molecular orbitals were calculated, Compton profiles and their anisotropies were deduced similarly to in the above case. Here, calculations were performed only on the valence electrons (the frozen-core approximation) as usual in pseudopotential calculations, whereas all the electrons were included in the Hartree–Fock calculation. The frozen-core approximation has no consequence for the anisotropies as the momentum distribution of core electrons has no directional dependency.

3.2. Band calculation

The present band calculation is based on the norm-conserving pseudopotential method [17] within the LDA framework [18, 19]. We used pseudopotentials proposed by Troullier and Martins [20] with the separable approximation [21] and the partial-core correction [22]. To obtain the final converged wave function, the preconditioned conjugate gradient method [23] modified by Bylander *et al* [24] with the charge-mixing scheme given by Kerker [25], which has been shown to be suitable for large metallic systems [26], was used together with the Gaussian-smearing technique [27]. The energy cut-off of the plane waves was chosen to be 57.5 Ryd. We determined this value by investigating the total-energy convergence for boron nitride. Nitrogen requires the highest energy cut-off among the elements in TTF-TCNQ. We used 64 $\boldsymbol{k}$-points in the irreducible zone (1/4 of the Brillouin zone) to ensure that we had the fine mesh of the momentum space needed for Compton-profile calculations, although we confirmed that eight $\boldsymbol{k}$-points are enough for obtaining the self-consistent charge. A quasi-one-dimensional electronic structure has been obtained as expected. The details of the band calculation will be published elsewhere. Compton profiles were calculated according to equations (1)–(4) and their anisotropies were obtained. In this case, j is a band label. Again, only valence electrons were included in the calculations.

4. Results and discussion

In figure 1, the anisotropies of the Compton profiles for the experiment and the three different calculation methods are shown. As for the Hartree–Fock molecular orbital calculation, the results obtained with the most precise 6-31G** basis set are shown.

First, we compare the results of the Hartree–Fock molecular orbital calculation with the experimental ones. All features appearing in the experimental anisotropies are reproduced in the calculated ones. Not only qualitative but also quantitative agreement is obtained. Disagreement is limited to small discrepancies in the positions of peaks and dips. The situation is the same for the LDA pseudopotential molecular orbital calculation. In spite of the quite different calculation schemes, these two methods give similar results. This confirms the validity of each calculation. The discrepancies between the experiment and the molecular orbital calculations should probably be ascribed to the crystallization effect, which is taken into account in the band calculation.

Before referring to the results of the band calculation, we would like to mention the results of the Hartree–Fock molecular orbital calculations with the other three basis sets. Calculated anisotropies are shown in figure 2. The result with the 6-31G basis set is very similar to that with 6-31G** shown in figure 1. The 3-21G basis set also provides a rather good agreement though it somewhat underestimates the magnitude of the anisotropies. The STO-3G set gives a poor agreement, especially in the low-momentum region for the c^*–b and b–a profiles. This might be due to the rigidity of the wave functions in this basis set where the orbitals have a fixed shape, while they are expressed by two groups of Gaussians for the other basis sets used

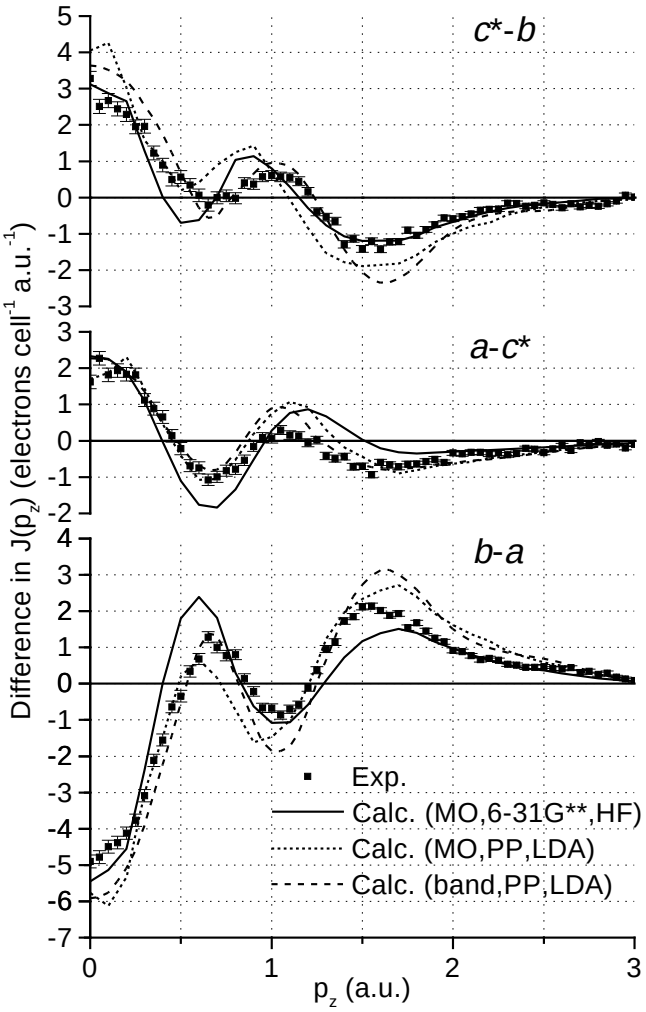

Figure 1. Anisotropies of the Compton profiles for TTF-TCNQ: experiment (squares), Hartree–Fock (HF) molecular orbital (MO) calculations with 6-31G** (solid line), LDA plane-wave pseudopotential (PP) molecular orbital (MO) calculations (dotted line) and LDA plane-wave pseudopotential (PP) band calculations (dashed line).

in the present work. In the latter case, the shape of the orbital can be tuned by changing the linear-combination coefficients of two Gaussians. These results show that Compton-profile studies provide a new and direct way to evaluate the Gaussian basis sets, by comparing the shapes of the momentum wave functions, not only for simple materials but also for complex compounds. This is a more stringent test of the calculation than a comparison with excitation energies, vibration frequencies or bond lengths, which has been the standard approach until now.

The Compton-profile anisotropies obtained by the band calculation are shown in figure 1 as dashed lines. The agreement of the peak and dip positions is much improved though the estimated amplitude is slightly higher than the experimental one. The pseudopotential technique neglects oscillatory behaviour of the wave function in the core region [17]. This means that the higher-momentum part of the Compton profile is strongly underestimated. This effect results in an overestimation of the amplitude in the low-momentum region through the normalization process [28]. In addition, the correlation effects may cause a weight transfer from lower to higher momenta [29]. Neglect of this leads to a similar overestimation in the

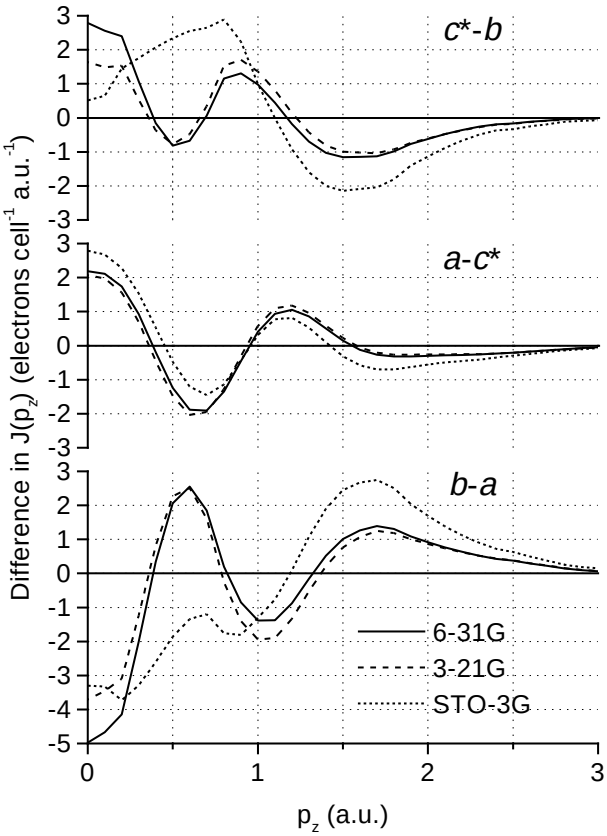

Figure 2. Anisotropies of the Compton profiles for TTF-TCNQ calculated with the 6-31G (solid line), 3-21G (dashed line) and STO-3G (dotted line) basis sets.

lower-momentum region. The c^*–b and b–a anisotropies should, in principle, contain Fermi-surface-related structures but these are too small in magnitude to be detected experimentally.

Though it appears that the electronic wave functions in the crystal TTF-TCNQ are well described with the superposition of those of the constituent molecules, the *ab initio* band calculations provide the more accurate result for the anisotropies. What is the origin of the difference between the band and molecular orbital calculations? One possible candidate is the charge transfer from TTF to TCNQ. However, this is not enough to explain the observed difference. Even if the contribution from the topmost bands derived from the TTF-HOMO and TCNQ-LUMO is removed, the difference in the anisotropy still exists. The contribution from these bands to the anisotropy is small.

Effects of the charge transfer are not limited to these topmost bands. To screen the transferred charge, the wave functions of the electrons in the remaining bands are also deformed. Since the Gaussian and plane-wave basis sets give very different wave functions in the core region, it is better to compare with the results from the same plane-wave basis set. We computed charge densities for the plane-wave pseudopotential molecular orbital calculation (MO, PP) and the band calculation (band, PP). Figure 3 represents the projection of the charge-density difference onto the a–c plane:

$$D_\rho(x, z) = \int (\rho_{\mathrm{band,PP}}(\boldsymbol{r}) - \rho_{\mathrm{MO,PP}}(\boldsymbol{r}))\, \mathrm{d}y. \tag{5}$$

Only the 122 bands which are fully occupied were taken into account. In the band calculation, the electron density at the TTF centre part (the C=C double bond) is higher while it is lower

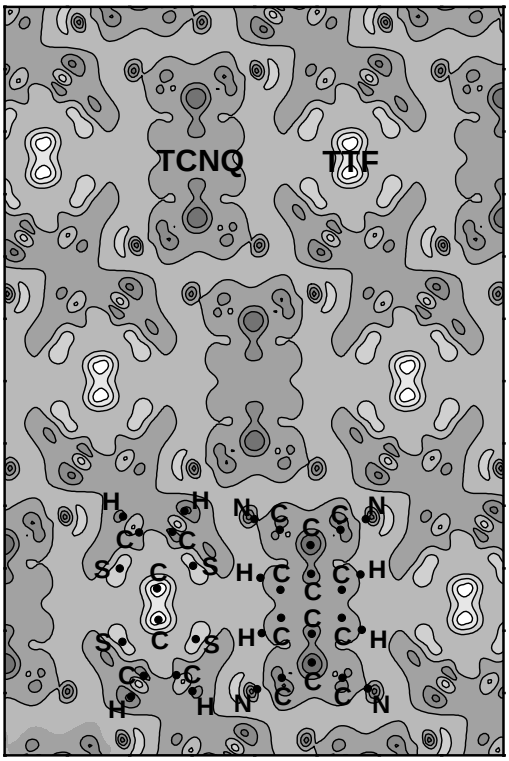

Figure 3. Projection of the charge-density difference between $\rho_{\mathrm{band,PP}}$ and $\rho_{\mathrm{MO,PP}}$ onto the a–c plane. Values range from -1.75×10^{-2} (dark) to $+2.12 \times 10^{-2}$ (bright) electrons au^{-2}.

at the C atoms of TCNQ between the CN groups. These positions correspond to the maxima of the TTF-HOMO and the TCNQ-LUMO. It is well known that, influenced by the charge transfer between these two orbitals, the wave functions for the remaining orbitals (bands) are deformed. Though the charge density does not directly correspond to the momentum density, it is expected that the wave-function deformation induces changes not only in the charge density but also in the momentum density.

There is another possible contribution to the difference between the molecular orbital and band calculations. By forming bands, the shapes of wave functions can be deformed in a manner which depends on $\boldsymbol{k}$. In other words, the wave functions have a dispersion. We found that this effect is significant only along the b-direction, reflecting the magnitude of inter-molecular overlaps.

5. Conclusions

We have successfully measured directional Compton profiles from TTF-TCNQ single crystals. Significant anisotropies are observed. The profiles and the anisotropies were first compared to theoretical calculations in which molecular orbitals have been described by Gaussian basis sets. The degree of the agreement between the experiment and the calculation depends on the basis set used in the calculation, demonstrating that Compton scattering can be efficiently used to evaluate the accuracy of the electron wave functions used in molecular orbital calculations. Except for the least accurate basis set STO-3G, reasonable agreement is obtained although the superposition of the molecular orbitals was used to express the electron wave function in the crystal. The molecular orbital calculation with the LDA pseudopotential method gave a

similar result. The remaining small deviations of the peak and dip positions in the anisotropies disappear in the *ab initio* pseudopotential band calculation. It is found that two major changes in the electronic structure occur in the solid state. One is the charge transfer from the TTF-HOMO to TCNQ-LUMO accompanied with charge redistribution to screen it. The other is the band dispersion of the wave functions along the conducting *b*-direction. The measured Compton-profile anisotropies reflect these electronic changes.

Acknowledgments

The authors are grateful to Professor M Peter and Professor Ø Fischer for their continuous encouragement and to Dr N Orita, Dr T Miyazaki and Dr H Katagiri for helpful discussion. All the calculations were performed utilizing computing resources at the Tsukuba Advanced Computing Centre (TACC), AIST, MITI.

References

[1] Manninen S, Honkimäki V, Hämäläinen K, Laukkanen J, Blaas C, Redinger J, McCarthy J and Suortti P 1996 *Phys. Rev.* B **53** 7714
[2] Ferraris J P, Cowan D O, Walatka V Jr and Perlstein J H 1973 *J. Am. Chem. Soc.* **95** 948
[3] Cohen M J, Coleman L B, Garito A F and Heeger A J 1974 *Phys. Rev.* B **10** 1298
[4] Ishiguro T and Yamaji K 1990 *Organic Superconductors* (Berlin: Springer)
[5] Williams J M, Ferraror J R, Thorn R J, Carlson K D, Geiser U, Wang H H, Kini A M and Wangbo M-H 1992 *Organic Superconductors* (Englewood Cliffs, NJ: Prentice-Hall)
[6] Kistenmacher T J, Phillips T E and Cowan D O 1974 *Acta Crystallogr.* B **30** 763
[7] Kagoshima S, Ishiguro T and Anzai H 1976 *J. Phys. Soc. Japan* **41** 2061
[8] Chiba T 1976 *J. Chem. Phys.* **64** 1182
[9] Chiba T 1992 *J. Phys. Chem. Solids* **53** 1677
[10] Shitzkovsky S, Weger M and Gutfreund H 1978 *J. Physique* **39** 711
[11] Frisch M J, Trucks G W, Schlegel H B, Gill P M W, Johnson B G, Robb M A, Cheeseman J R, Keith T, Petersson G A, Montgomery J A, Raghavachari K, Al-Laham M A, Zakrzewski V G, Ortiz J V, Foresman J B, Peng C Y, Ayala P Y, Chen W, Wong M W, Andres J L, Replogle E S, Gomperts R, Martin R L, Fox D J, Binkley J S, Defrees D J, Baker J, Stewart J P, Head-Gordon M, Gonzalez C and Pople J A 1995 *Gaussian 94, Revision B.3* (Pittsburgh, PA: Gaussian Incorporated)
[12] Ishibashi S, Manuel A A, Hoffmann L and Bechgaard K 1997 *Phys. Rev.* B **55** 2048
[13] Hehre W J, Stewart R F and Pople J A 1969 *J. Chem. Phys.* **51** 2657
[14] Binkley J S, Pople J A and Hehre W J 1980 *J. Am. Chem. Soc.* **102** 939
[15] Hehre W J, Ditchfield R and Pople J A 1972 *J. Chem. Phys.* **56** 2257
[16] Hariharan P C and Pople J A 1973 *Theor. Chim. Acta* **28** 213
[17] Hamann D R, Schlüter M and Chiang C 1979 *Phys. Rev. Lett.* **43** 1494
[18] Ceperley D M and Alder B J 1980 *Phys. Rev. Lett.* **45** 566
[19] Perdew J P and Zunger A 1981 *Phys. Rev.* B **23** 5048
[20] Troullier N and Martins J L 1991 *Phys. Rev.* B **43** 1993
[21] Kleinman L and Bylander D M 1982 *Phys. Rev. Lett.* **48** 1425
[22] Louie S G, Froyen S and Cohen M L 1982 *Phys. Rev.* B **26** 1738
[23] Teter M P, Payne M C and Allan D C 1989 *Phys. Rev.* B **40** 12 555
[24] Bylander D M, Kleinman L and Lee S 1990 *Phys. Rev.* B **42** 1394
[25] Kerker G P 1981 *Phys. Rev.* B **23** 3082
[26] Kohyama M 1996 *Modell. Simul. Mater. Sci. Eng.* **4** 397
[27] Fu C-L and Ho K-M 1983 *Phys. Rev.* B **28** 5480
[28] Delaney P, Králik B and Louie S G 1998 *Phys. Rev.* B **58** 4320
[29] Králik B, Delaney P and Louie S G 1998 *Phys. Rev. Lett.* **80** 4253